FULL LENGTH ARTICLE

The Anatomical Record
Advances in Integrative Anatomy and Evolutionary Biology

WILEY

Postnatal ontogeny of the femur in fossorial and semiaquatic water voles in the 3D-shape space

Ana Filipa Durão[1] | Francesc Muñoz-Muñoz[1] | Jacint Ventura[1,2]

[1]Departament de Biologia Animal, de Biologia Vegetal i d'Ecologia, Facultat de Biociències, Universitat Autònoma de Barcelona, Campus de Bellaterra, Cerdanyola del Vallès, Spain

[2]Àrea de recerca en petits mamífers, Museu de Ciències Naturals de Granollers "La Tela", Barcelona, Spain

Correspondence
Ana Filipa Durão and Francesc Muñoz-Muñoz, Departament de Biologia Animal, de Biologia Vegetal i d'Ecologia, Facultat de Biociències, Universitat Autònoma de Barcelona, Campus de Bellaterra, 08193 Cerdanyola del Vallès, Spain.
Email: anafilipa.lopes@uab.cat (A. F. D.) and francesc.munozm@uab.cat (F. M.-M.)

Funding information
Comissionat per a Universitats i Recerca (Generalitat de Catalunya), Grant/Award Number: 2014-SGR-1241

Abstract

Water voles of the genus *Arvicola* constitute an excellent subject to investigate to which extent function affects postnatal developmental growth of limb structures in phylogenetically close species. We performed a comparative analysis of postweaning femur form changes between *Arvicola sapidus* (semiaquatic) and *Arvicola scherman* (fossorial) using three-dimensional landmark-based geometric morphometrics. In both species, we observed greater femur robustness in juvenile individuals than in adult ones, probably due to the accommodation of high loads on the bone during initial locomotor efforts. Significant interspecific differences were also found in the femur size and shape of adult specimens, as well as in the postnatal allometric and phenotypic trajectories. In terms of phenotypic variation, fossorial water voles show relatively wider third and lesser trochanters, and greater femur robustness than *A. sapidus*, characters associated to the digging activity. In contrast, *A. sapidus* displays a slight increase of the greater trochanter in comparison with *A. scherman*, which is seemingly an adaptive response for enhancing propulsion through the water. Results evidence that certain morphological traits and differences between *A. sapidus* and *A. scherman* in the allometric and phenotypic trajectories of the femur are associated with their different locomotor mode.

KEYWORDS
allometry, *Arvicola*, locomotion, ontogenetic pattern, phenotypic trajectories

1 | INTRODUCTION

Over the past decades, extensive work has been done on the role played by the locomotor behavior on the phenotypic variation of limb long bones in rodents (Durão, Muñoz-Muñoz, & Ventura, 2020; García-Esponda & Candela, 2016; Hildebrand, 1985; Lehmann, 1963; Lessa, Vassallo, Verzi, & Mora, 2008; Samuels & Valkenburgh, 2008; Stein, 1993, 2000). Notably, it has been shown that different locomotion modes may lead to profound changes in the architecture of the myoskeletal system (Candela & Picasso, 2008; Lessa et al., 2008; Salton & Sargis, 2009; Sargis, 2002). Moreover, ecological factors, functional constraints, or evolutionary adaptations can be associated with modifications of the postnatal developmental pathways of the corresponding bone structures (Adams & Nistri, 2010; Durão et al., 2020; Durão, Ventura, & Muñoz-Muñoz, 2019; Esquerré, Sherratt, & Keogh, 2017; Gray, Sherratt, Hutchinson, & Jones, 2019; Wilson & Sánchez-Villagra, 2010). In this context, a

comparison of the ontogenetic trajectories of limb long bones of closely related species with different locomotor types is an excellent way to determine to which extent function affects growth patterns. Within rodents, water voles of the Palaearctic genus *Arvicola* constitute an optimal subject to explore this issue since it comprises a high number of morphotypes and two main ecological forms, semiaquatic, and fossorial.

The phylogenetic relationships of the representatives of *Arvicola* are currently under debate. Classically two species within this genus were recognized (see, e.g., Reichstein, 1963, 1982): *Arvicola sapidus*, which comprises semiaquatic populations, and *Arvicola terrestris*, with fossorial and/or semiaquatic representatives. In the taxonomic review of this genus by Musser and Carleton (2005), three species were accepted: the southwestern water vole, *A. sapidus* Miller, 1908 (semiaquatic); the montane water vole, *Arvicola scherman* (Shaw, 1801) (fossorial); and the European water vole, *Arvicola amphibius* (Linnaeus, 1758) (semiaquatic or mostly semiaquatic). Although *A. sapidus* is widely accepted as a valid species, recent studies based on analyses of genetic data have given rise to controversy on the taxonomy of the formerly accepted *A. terrestris* (for details, see Chevret et al., 2020; Kryštufek et al., 2015; Mahmoudi et al., 2020; Pardiñas et al., 2017; Ventura & Casado-Cruz, 2011 and references therein). As for the Iberian populations analyzed in the present study, according to these new results, fossorial water voles from the Pyrenees could be attributed to *A. amphibius* sensu *lato* (Kryštufek et al., 2015), *Arvicola monticola* (Mahmoudi et al., 2020; Pardiñas et al., 2017) or *A. amphibius* (Chevret et al., 2020). Since this point remains unsolved, we decided to follow the taxonomic arrangement by Musser and Carleton (2005) to clearly distinguish between typical fossorial (*A. scherman*) and semiaquatic (*A. sapidus*) morphotypes.

Fossorial water voles exhibit the so-called chisel tooth digging, which involves the use of procumbent incisors to break the soil (Stein, 2000). The soil loosened by the incisors is removed from the tunnel through rapid and alternative movements of the fore and hind limbs, and the gallery walls are compacted by the rostrum (Airoldi, Altrocchi, & Meylan, 1976; Laville, 1989; Laville, Casinos, Gasc, Renous, & Bou, 1989). This digging process allows *A. scherman* to build extensive and complex burrow systems in hard soils (Airoldi, 1976; Airoldi & De Werra, 1993; Laville, 1989). Conversely to fossorial water voles, *A. sapidus* lives in freshwater habitats where it builds burrows on easily penetrable soils (Ventura, 2007). These rodents are excellent swimmers and divers (Mate, Barrull, Salicrú, Ruiz-Olmo, & Gosàlbez, 2013; Quéré & Le Louarn, 2011) albeit they do not show marked morphological characteristics associated with these activities.

During swimming, *A. sapidus* uses fore and hind limbs to move quickly in water and with hind limbs to generate propulsion. Thus, in *A. scherman* and *A. sapidus*, hind legs are employed differently, according to their dominant type of locomotion. On the one hand, fossorial water voles mainly use their hindlimbs to remove the soil from the burrow (see Airoldi et al., 1976). During this phase, the animal takes a flexed posture; the pelvis is tilted forward, the angle between the femur and the pelvis diminishes, and the thigh is extended backward (Laville, 1989). On the other hand, as mentioned above, semiaquatic water voles use hind legs to generate propulsion during swimming. Specifically, *A. sapidus* places first the hind feet ventrally and then extends the hip and knee. In this process, the femur is essential to make rapid movements and to exert force during the legs' stroke.

Despite the important role that the hindlimbs play in the different locomotion modes in *Arvicola*, little is known about the postnatal development of their bones (Garde, 1992; Ventura, 1988, 1990, 1992). Surprisingly, this observation can be also extended to rodents in general (Elissamburu & Vizcaíno, 2004; Laville, 1989; Montoya-Sanhueza, Wilson, & Chinsamy, 2019; Samuels & Valkenburgh, 2008; Stein, 1993). The present study is the third one of a series that aimed to determine the postnatal development of bone structures involved in locomotion in the two ecological forms of *Arvicola*: fossorial and semiaquatic. The main goal of this research is to compare the postnatal ontogeny of the femur in *A. scherman* (fossorial) and *A. sapidus* (semiaquatic) to detect possible phylogenetic and functional signals in this process. We compared the vectors of growth trajectories to estimate whether evolved functional differences are associated with different ontogenetic patterns. We hypothesize that these species share conserved shape changes throughout their postnatal growth. However, considering the corresponding type of locomotion, we also expect significant interspecific differences both in the allometric and phenotypic trajectories. This hypothesis is supported by our previous results obtained for the mandible (Durão et al., 2019) and humerus (Durão et al., 2020) of these taxa. It is worth mentioning that although there is available information on the postweaning development of the femur in scratch digger rodents (Echeverría, Becerra, & Vassallo, 2014; Montoya-Sanhueza et al., 2019; Vassallo, 1998), here we give the first findings on this subject concerning a chisel-digger vole (*A. scherman*). The results obtained in *A. scherman* were compared, under a functional perspective, with those corresponding to a typical semiaquatic species of the same genus (*A. sapidus*).

2 | MATERIALS AND METHODS

2.1 | Study specimens

We studied ontogenetic series of two *Arvicola* representatives: *A. sapidus* and *A. scherman*. The analyzed sample (Table 1) consisted of 182 right femora from museum collections, 89 belonging to *A. sapidus* from the Ebro Delta (Tarragona, Spain), and 93 to *A. scherman* from the Aran Valley (Lleida, Spain). Due to the small number of juvenile *A. sapidus* in this sample, we complemented it with femurs of juvenile individuals from Mélida (Navarra, Spain) collected in 1990, and Banyoles (Girona, Spain) and Rieutort (Lozère, France) obtained in 1994. Results of previous studies showed no significant morphometric differences between these populations (Garde, 1992; Ventura, 1988).

We analyzed specimens belonging to the same collections examined in previous comparative studies on the ontogeny of the mandible (Durão et al., 2019; Ventura & Casado-Cruz, 2011) and humerus of these species (Durão et al., 2020). As in the case of these bones, those specimens were already distributed into six classes of relative age according to criteria based on the moulting phase, sexual stage, and skull morphology (for details, see Garde, Escala, & Ventura, 1993; Ventura & Gosálbez, 1992). The age intervals corresponding to each group are the following (Garde et al., 1993; Ventura & Gosálbez, 1992): Class 0, 3 weeks maximum; Class 1, between 3 and 5 weeks; Class 2, between 6 and 10 weeks; Class 3, between 10 and 14 weeks; Class 4, between 14 weeks and 1 winter; and Class 5, individuals that have lived more than 1 winter. Individuals from the last two age classes were considered fully adults.

Excepting the femurs of *A. sapidus* from Mélida, all material analyzed in the present study is provisionally housed in the collection from the Mammalian Biology Research Group of the Universitat Autònoma de Barcelona (UAB, Bellaterra, Spain). Specimens from Mélida belong to the collection of the Museo de Ciencias of the Universidad de Navarra (UNAV, Pamplona, Spain). Catalogue numbers of museum material are in Appendix.

2.2 | Femur form

2.2.1 | Three-dimensional (3D) models

Femur form variation was studied from 3D models obtained by the photogrammetric technique, which permits to obtain accurate and precise models of the external form of small objects from photograph sets (Durão, Muñoz-Muñoz, Martínez-Vargas, & Ventura, 2018). Each model was constructed from a set of 33 photographs of each femur using a Canon EOS 750D DSLR camera equipped with a Tamron 60 mm f/2.0 Di II LD macro lens and a polarizing filter mounted on a tripod. The models were obtained through the "turntable method," which consists of keeping the camera fixed at a point and taking photographs of the object while it rotates on a turntable in small intervals. All photographs were taken inside a lightbox to even out the light and reduce gleams and harsh changes in shadows during the rotation of the specimen. In order not to obstruct viewing angles and to obtain a complete digital model, the photographs were taken at intervals of 15° (Falkingham, 2012). Thus, photographs were taken in two complete rotations of 360°: the first rotation at the same height as the bone (taking 24 photos at intervals of 15°) and the second rotation at the height of bone size, positioning the lens at 20° from the horizontal plane (taking 9 photos at 40° intervals). Each photo was taken via remote trigger to reduce camera shake while capturing images and get focused and sharped photos. Internal software parameters, such as total error and residual and precision values, were used to assess the quality of the models. For more details about the protocol, see Durão et al. (2018).

2.2.2 | Morphometric data

The femur form was characterized using 3D landmark-based geometric morphometrics. A set of 20 landmarks (Figure 1) were digitized on the femur surface using Photomodeler Scanner software v.2015.1.1 (EOS Systems Inc., 2015). Landmark definition is available in

TABLE 1 Sample size for each species, age class, and sex

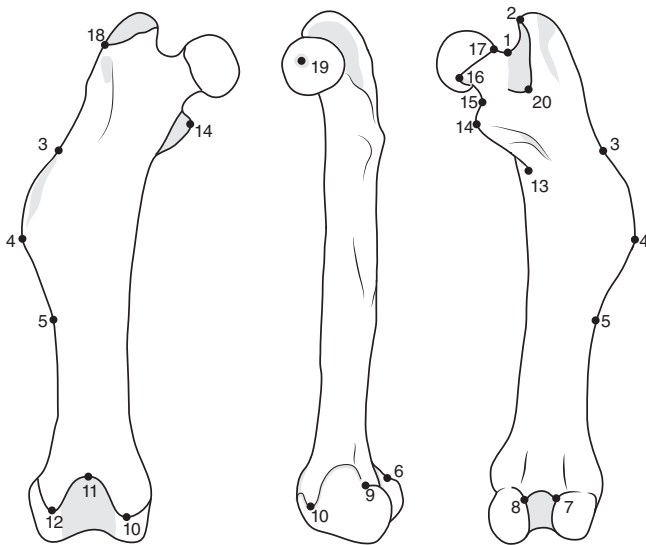| Species | Sex | Age class | | | | | | Total |
		0	1	2	3	4	5	
Arvicola sapidus	F	2	10	9	3	9	4	89
	M	3	10	8	10	9	12	
Arvicola scherman	F	2	5	10	10	10	10	93
	M	4	2	10	10	10	10	
Total		11	27	37	33	38	36	182

FIGURE 1 Femur image of *Arvicola scherman* showing the position of the 20 anatomical landmarks used in the geometric morphometric analyses, from left to right: cranial, medial, and caudal. See Table S1 for landmark definitions

Supplementary Material S1. We set the scale for each model using the mean value of the three measurements of the linear distance between points 2 and 11. Measurements were obtained with a Mitutoyo 500-161-21 Digital Caliper (Mitutoyo America Corporation, Aurora, IL) with a 0.01 mm resolution. To avoid interobserver error, all femur digitalization was taken by the same person (A.F.D.). Subsequent analyses were performed using MorphoJ v.1.07a (Klingenberg, 2011) and a routine written for R statistical framework v. 4.1.0 (R Development Core Team, 2016).

Femoral form was separated into size and shape components, which were analyzed separately. Centroid size, defined as the square root of the sum of the square distances of each landmark from their centroid (Bookstein, 1991), was used as a proxy for femur size. The raw 3D landmarks coordinates were subjected to a generalized Procrustes alignment (Rohlf & Slice, 1990) to remove nonshape information (size, position, and orientation) (Dryden & Mardia, 1998; Goodall, 1991). Thus, the isometric effect of size on shape was removed but not allometry. The resulting Procrustes coordinates were used as shape variables in further analyses.

2.3 | Statistical analyses

2.3.1 | Sexual dimorphism

We assessed the presence and magnitude of sexual dimorphism in each species on femur size and shape performing a factorial analysis of variance (ANOVA) and a Procrustes ANOVA, respectively. The factorial ANOVA was conducted with sex and age class as categorical factors and log-transformed centroid size (LCS) as dependent variable. In the case of Procrustes ANOVA, sex was introduced as categorical factor, LCS as continuous variable and Procrustes coordinates as dependent variables. No sexual dimorphism was found in any species (Supplementary Material - Tables S2–S5), which corroborates results obtained in other studies (Garde, 1992; Ventura, 1988, 1990, 1992, 1993; Ventura & Casado-Cruz, 2011). Consequently, for each species data from both sexes were analyzed together.

2.3.2 | Size and allometry

For both *A. sapidus* and *A. scherman*, the mean LCS and the respective standard deviations for each age class were computed. The effects of species and age classes on femur size were tested across the entire sample with a factorial ANOVA. To test for differences between species in each age class, a Tukey's HSD test was applied. To reduce the occurrence of a type-I error in sets of related tests, a sequential Bonferroni correction was conducted (Rice, 1989). These analyses were carried out using STATISTICA v.12 software (StatSoft, 2014).

The statistical relationship between size and shape (allometry) was assessed for each species separately by multivariate regression of Procrustes coordinates on LCS (Monteiro, 1999). Statistical significance of the results was tested under the null hypothesis of no allometric relationship through a permutation test with 10,000 iterations. These analyses were performed with MorphoJ v.1.07a. A Procrustes ANOVA model using LCS, species and their interaction as model effect (Goodall, 1991) was conducted to estimate the allometric relationship between species, by means of the "procD.lm" function from the R package geomorph (Adams, Collyer, Kaliontzopoulou, & Sherratt, 2017). The statistical significance was assessed via distributions generated with resampling permutation with 10,000 iterations (Collyer, Sekora, & Adams, 2015). In this ANOVA, the significant interaction between species and LCS suggests interspecific differences in allometry. Since this was the case (see the Results section), to evaluate differences in ontogenetic allometric patterns, the attributes of the vectors of allometric coefficients, length (magnitude), and orientation (angle) were computed applying the "pairwise" function from the package RRPP (Collyer & Adams, 2018). Vector length describes the amount of shape changes per unit change of size and vector orientation indicates the relative covariations of shape variables per unit change of size (Collyer & Adams, 2013). Statistical significance of the tests was via pairwise assessments of the similarity in slopes and through 10,000 randomized residual permutations.

2.3.3 | Shape variation

A principal component analysis (PCA) on Procrustes aligned coordinates was performed to investigate the variation among landmarks in the data set. To visualize the shape differences associated with the major principal components (PCs), a warped 3D model was produced using plotRefToTarget function from R package geomorph (Adams et al., 2017). To measure similarity and difference between species, we calculated Procrustes distances from shape data and nonallometric shape data (allometric shape removed) in each age class. The residuals obtained from the multivariate regression of Procrustes coordinates on LCS for each age class of each species were used as non-allometric shape data (see Klingenberg, 2016). Sequential Bonferroni corrections were applied. Femur shape differences across ontogeny between *A. sapidus* and *A. scherman* were visualized by discriminant analysis (DA) performed in two separate groups of individuals: juvenile and subadult (age classes 0–3), and adult (age classes 4 and 5). All the described analyses were conducted with MorphoJ v.1.07a. The resulting coordinates of this difference were imported and used in plotRefToTarget function to visualize the differences between species.

To compare ontogenetic trajectories between species, a phenotypic trajectory analysis (PTA) on the Procrustes coordinates, using the "trajectory.analysis" function from the RRPP, was conducted (Adams & Collyer, 2007, 2009; Collyer & Adams, 2007, 2013). This function quantifies the attributes of the phenotypic trajectories (size, orientation, and shape) for each group and compares these attributes between groups via permutation (Adams & Collyer, 2009). We used species as group and age class as the trajectory points. Attribute differences were estimated from sampling distributions generated from 10,000 random residual iterations (Adams & Collyer, 2007, 2009; Collyer & Adams, 2007, 2013). To visualize the ontogenetic phenotypic trajectories, a PC of fitted values from linear model fit over multiple random permutations was computed (Adams & Collyer, 2009). To visualize shape changes, a warped 3D model was plotted. To ensure that the low sample size of Classes 0 and 1 did not influence the PTA, the same analysis was performed without these two age classes.

3 | RESULTS

3.1 | Size and allometry

The factorial ANOVA indicated that femur size was significantly influenced by species, age class, and the interaction of both factors (Table 2). Femur size increased

TABLE 2 Results of the factorial ANOVA testing the effects of species, age class, and the interaction between them on femur size (logarithm of centroid size)

Effect	df	SS	MS	F	p
Species	1	3.951	3.951	1,566.2	<.001
Age class	5	4.204	0.841	333.3	<.001
Age class × species	5	0.044	0.009	3.5	.005
Residuals	170	0.429	0.003		

Abbreviations: *df*, degrees of freedom; *F*, F statistic; MS, mean squares; *p*, *p*-value; SS, sum of squares.
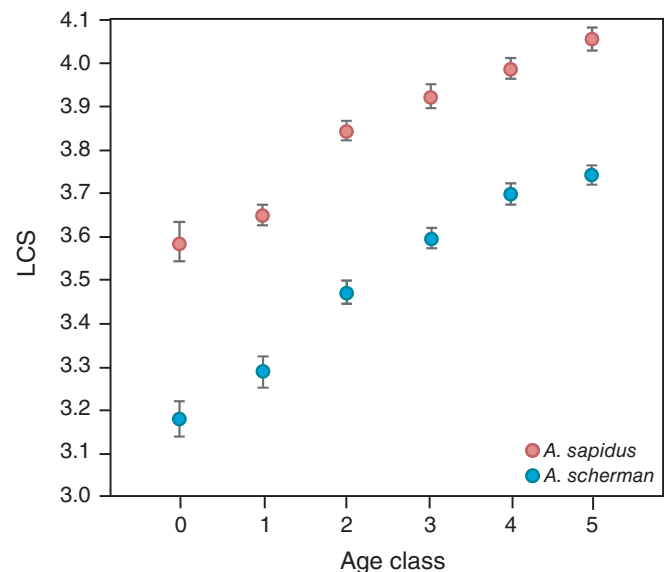

FIGURE 2 Mean values of the logarithm of centroid size (LCS) of the femur across the ontogeny in *Arvicola sapidus* and *Arvicola scherman* (whiskers, standard deviation)

throughout ontogeny in both species (Figure 2), although it was always larger in *A. sapidus* than in *A. scherman* (Table 3). Multivariate regression of Procrustes coordinates on LCS for each species revealed that both species show significant shape changes, in *A. sapidus* the size explained 38.52% of the shape variation and in *A. scherman* 27.88% (Figure 3).

Species, size, and their interaction had a significant effect on femur shape (Table 4). Thus, there was allometry in femur shape and the significant interaction term suggests that the allometric slopes of these species were significantly different. Pairwise comparison of allometric trajectories confirmed that allometric slopes significantly differed between species ($\theta = 26.02°$; $p < .001$). No significant pairwise difference in trajectory length was detected ($\Delta d = 0.017$; $p = .06$), but *A. sapidus* displayed a longer vector than *A. scherman* ($d_{A. \, sapidus} = 0.186$; $d_{A. \, scherman} = 0.169$).

	Centroid size		
Age class	*Arvicola sapidus*	*Arvicola scherman*	*p*-values*
0	35.49 ± 0.92	24.08 ± 0.84	<.001
1	38.64 ± 0.46	28.09 ± 0.77	<.001
2	46.68 ± 0.50	32.25 ± 0.46	<.001
3	50.44 ± 0.57	36.38 ± 0.46	<.001
4	53.76 ± 0.48	40.27 ± 0.46	<.001
5	57.56 ± 0.51	42.09 ± 0.46	<.001
Mean	47.10 ± 0.24	33.86 ± 0.24	<.001

TABLE 3 Mean centroid size and standard deviation of the femur in *Arvicola sapidus* and *Arvicola scherman* in each age class and associated *p*-values

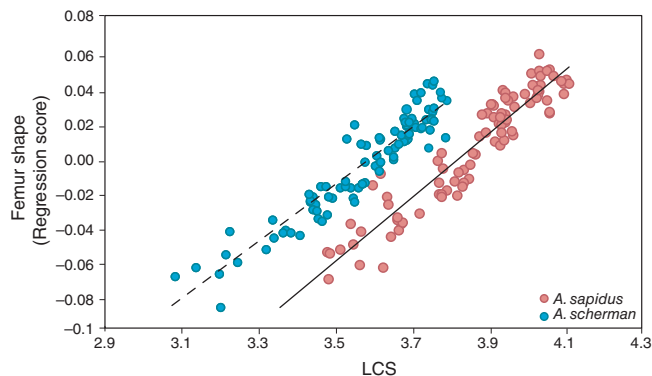*After sequential Bonferroni correction.

FIGURE 3 Multivariate regression of shape onto the logarithm of centroid size (LCS) in *Arvicola sapidus* and *Arvicola scherman* and their respective regression lines

3.2 | Variation in femur shape and phenotypic trajectories analyses

In the PCA of shape data, the first two PCs jointly explained 45.62% of overall variance (PC1 = 34.01%, PC2 = 11.61%) (Figure 4a). Each of the remaining PCs accounted for less than 6.7% of the variation (Table S6) and did not show a clear association with factors of interest. The shape changes explained by PC1 were mainly associated with age so that the youngest specimens showed positive values while the oldest ones showed negative values. The PCA that characterizes the general shape of the femur among specimens showed that younger individuals have high values of PC1 (Figure 4a). Increasing scores of PC1 involved a medial expansion of the femur's head (verifiable by a medial shift of the *fovea capitis*), distal expansion of the lesser trochanter, lateral expansion of the greater trochanter, shortening of the third trochanter, and a general expansion of the distal epiphysis. Specifically, the latter change included a medial expansion of medial condyle and medial epicondyle, and a lateral expansion of lateral condyle and lateral epicondyle (Figure 4b; Figure S1). The PC2 accounted for differences between the two species, with most *A. sapidus* specimens (excepting some adults) showing positive scores and most *A. scherman* individuals (excepting certain individuals of each age class) negative ones. Most individuals of *A. sapidus* (high PC2 values) have a slight reduction of the femur head (lateral shift of the *fovea capitis*) and a narrowing of the femur's neck, slight shortening of the greater and lesser trochanters, marked shortening and narrowing of the third trochanter, and distal expansion of both condyles (Figure 4c; Figure S1).

The DAs showed that both juveniles-subadult (age classes 0–3) and adult (age classes 4 and 5) individuals of *A. scherman* showed a more robust femur than *A. sapidus*. This robustness is mainly due to the expansion of the lesser trochanter, a slight medial shift of the femur head, relatively longer and prominent third trochanter, and medial expansion of both the medial epicondyle and medial condyle (Figures S2 and S3). In general, both species showed similar morphological changes between juvenile-subadult and adult stages (Figures S2a,b and S3a,b). In all age classes, both in shape data and in non-allometric shape data, Procrustes distances between species were significant (Table 5). These distances were always higher in nonallometric shape data.

Comparisons between the phenotypic trajectories (Figure 5) revealed significant differences between species in the direction (angle) of shape change ($\theta = 29.45°$; $p < .001$). However, neither the size (magnitude) ($\Delta d = 0.009$; $p = .36$ [$d_{A. sapidus} = 0.129$; $d_{A. scherman} = 0.138$]) nor the shape of the phenotypic trajectories ($D_p = 0.21$; $p = .08$) were significantly different between taxa. For PC1, both species trajectories run from lower values as juveniles to higher values as adults. Along PC2 there is a separation between trajectories, showing *A. sapidus* the highest scores. The variation detected in shape data by a PTA without age classes 0 and 1 was similar to that observed when considering all age classes (Table S7).

TABLE 4 Results of the Procrustes ANOVA testing the effects of logarithm of centroid size (LCS), species, and the interaction between them on shape conducted on the entire sample

Effect	df	SS	MS	Rsq	F	Z	p
LCS	1	0.135	0.135	0.254	73.899	5.319	<.01
Species	1	0.062	0.062	0.117	33.945	7.230	<.01
LCS × species	1	0.008	0.008	0.016	4.615	4.732	<.01
Residuals	178	0.325	0.002	0.613			
Total	181	0.530					

Abbreviations: *df*, degrees of freedom; *F*, *F* statistic; *MS*, mean squares; *p*, *p*-value; Rsq, R-squared values; SS, sum of squares; *Z*, effect-size.
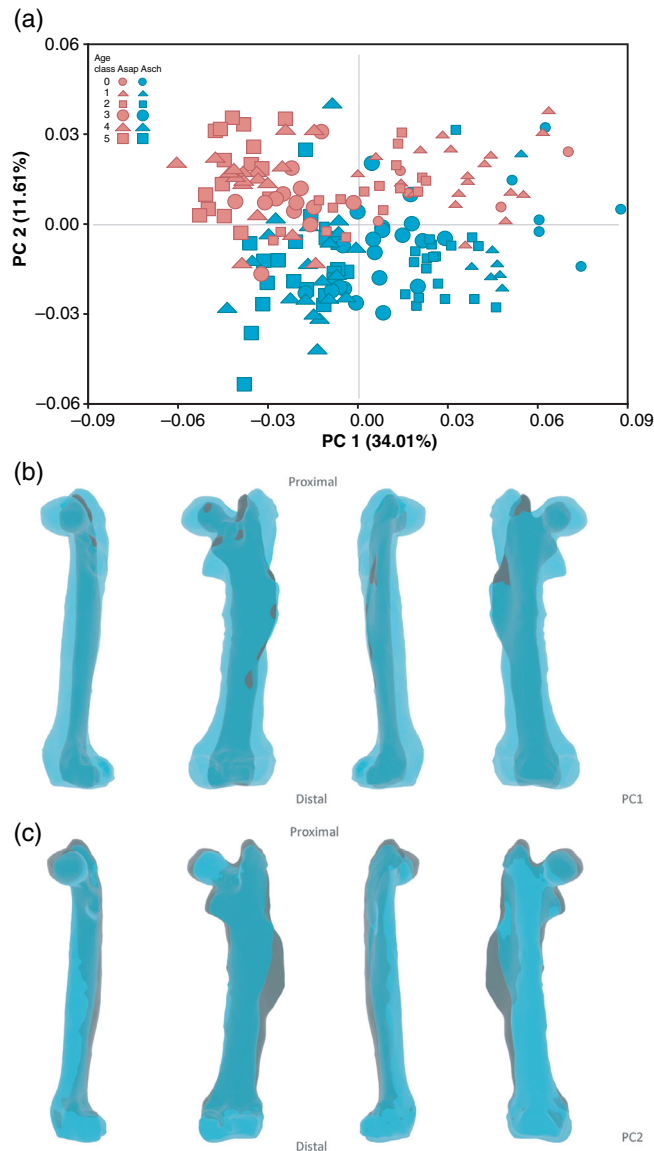

FIGURE 4 (a) Scatterplot of the first two principal components (PC1 and PC2) from the principal component analysis performed on Procrustes coordinates. (b, c) Shape changes associated with each extreme of the first two principal components; gray, negative extreme of the axis; blue, positive extreme of the axis. Bones are represented from left to right in medial, caudal, lateral, and cranial views

4 | DISCUSSION

4.1 | Common ontogenetic phenotypic changes in the femur of semiaquatic and fossorial water voles

In concordance with our hypothesis, the PCA revealed that the general pattern of femur shape variation during postnatal ontogeny is similar in *A. sapidus* and *A. scherman*. In particular, important shared morphological changes were observed in the epiphyses. The first PC showed that the proximal and distal epiphysis are relatively larger in young individuals than in adult ones. These features likely provide a more multiaxially mobile hindlimb to juvenile voles (Salton & Sargis, 2009). Results obtained in an experimental study on mice (Serrat, Lovejoy, & King, 2007) allow us to suggest that differences in the epiphyses shape between juvenile and adult water voles could be associated to age-related differences in the expression levels of several growth factors.

In addition, the femur is more robust in juvenile than in adult individuals. This is due, at least in part, to the increase in body mass that determines higher mechanical loads on the limb long bones (García & da Silva, 2006). A similar growth pattern was reported for the postweaning ontogeny of the humerus (Durão et al., 2020), according to which, regardless of the type of locomotion, both bones are more robust in young than in adult water voles. In rodents, limb long bones of juvenile individuals are generally composed of faster deposition tissues and poorly mineralized woven (Enlow, 1962; Montoya-Sanhueza & Chinsamy, 2018). In contrast, adult specimens are characterized by having a mature compact bone, formed by lamellar bone that acts as a fiber-reinforced composite material (Enlow, 1962; Montoya-Sanhueza & Chinsamy, 2018). Since the mechanical and structural properties of the bone determine the organism's response to a mechanical load (Hart et al., 2017 and references therein), robust limb long bones in young water voles might be a

| Age class | Procrustes distance | | | |
	Shape data	*p*-value*	Nonallometric shape data	*p*-value*
0	0.036	<.001	0.109	<.001
1	0.036	<.001	0.051	<.001
2	0.037	<.001	0.089	<.001
3	0.040	<.001	0.096	<.001
4	0.037	<.001	0.066	<.001
5	0.048	<.001	0.069	<.001

TABLE 5 Procrustes distance between *Arvicola sapidus* and *Arvicola scherman* in each age class and associated *p*-values

*After sequential Bonferroni correction.

compensatory response to minimize the risk of fractures during initial locomotor efforts. As pointed out for other mammal species (Carrier, 1983; Echeverría et al., 2014; Montoya-Sanhueza et al., 2019; Young, Férnandez, & Fleagle, 2010), this response in *Arvicola* is probably related to the weak bone matrix and lower muscular development characteristic of juvenile individuals.

4.2 | Differences in the postweaning growth of the femur between semiaquatic and fossorial water voles

4.2.1 | Size change

The femur size of *A. scherman* is significantly smaller than that of *A. sapidus* across the whole postnatal ontogeny, which is congruent with the body size relationship between both taxa. The relatively smaller body size of *A. scherman* appears to be an adaptive response to hypogeic life (Cubo, Ventura, & Casinos, 2006; Durão et al., 2019, 2020). Given that the burrowing cost is proportional to the volume of soil dug (Vleck, 1979), it is usually assumed that a decrease in body size achieves a reduction in burrow cross-section, and consequently a reduction of the locomotion cost. Since the digging activity requires high energy, a decrease in body size becomes an advantage for fossorial animals (White, 2005) allowing them to channel energy more efficiently.

4.2.2 | Shape change

The analysis of allometric trajectories revealed a significant difference in the direction of the vectors of allometric coefficients between *A. sapidus* and *A. scherman*, which indicates that allometry is a significant component of the femoral shape variation. Significant interspecific differences in the direction of the vectors of allometric coefficients have been previously reported in the mandible (Durão et al., 2019) and the humerus (Durão et al., 2020) (Table S7). No significant difference in the length of the vectors was found, which means that the amount of shape changes per size unit is equal in both taxa. The fact that both species have a similar magnitude of allometric shape changes in the femur may be due to the important involvement of the femur in corresponding types of locomotion from an early age. Specifically, very young individuals of *A. scherman* quickly show an identical digging behavior to adults (Airoldi et al., 1976). To our knowledge, the age at which southern water voles begin to swim has not been reported but personal observations (J.V.) suggest that this activity appears not too late after weaning. Although the mechanical action of the femur is different in digging and swimming, functional pressure can be alike (Salton & Sargis, 2009; Samuels, Meachen, & Sakai, 2013; Samuels & Valkenburgh, 2008; Smith & Savage, 1956) contributing to a similar magnitude of the femoral shape change during postnatal ontogeny in these species. The fact that the mandible and humerus play a preponderant role in the digging process makes the functional pressure produce important morphological changes in these bones in a short time. Since in *A. sapidus* these structures are not subjected to the same functional pressure, their age-related changes are not so rapid. Although, in semiaquatic species, such as *A. sapidus*, the femur plays an important role in swimming, in the tibia and metatarsals there are key changes associated with the generation of propulsion during the power stroke and with paddling during swimming (Samuels & Valkenburgh, 2008). This could justify why, unlike the femur, in the mandible (Durão et al., 2019) and the humerus (Durão et al., 2020) the length of the vectors also differed significantly between species.

It has been suggested that time is needed for changes in the direction of allometric trajectories to take place (Voje, Hansen, Egset, Bolstad, & Pélabon, 2013) due to the high costs to growth dynamics (Gould, 1966). However, several works have shown that ontogenetic trajectories themselves can evolve, being prone to selection and evolutionary change (Adams & Nistri, 2010; Gray et al., 2019;
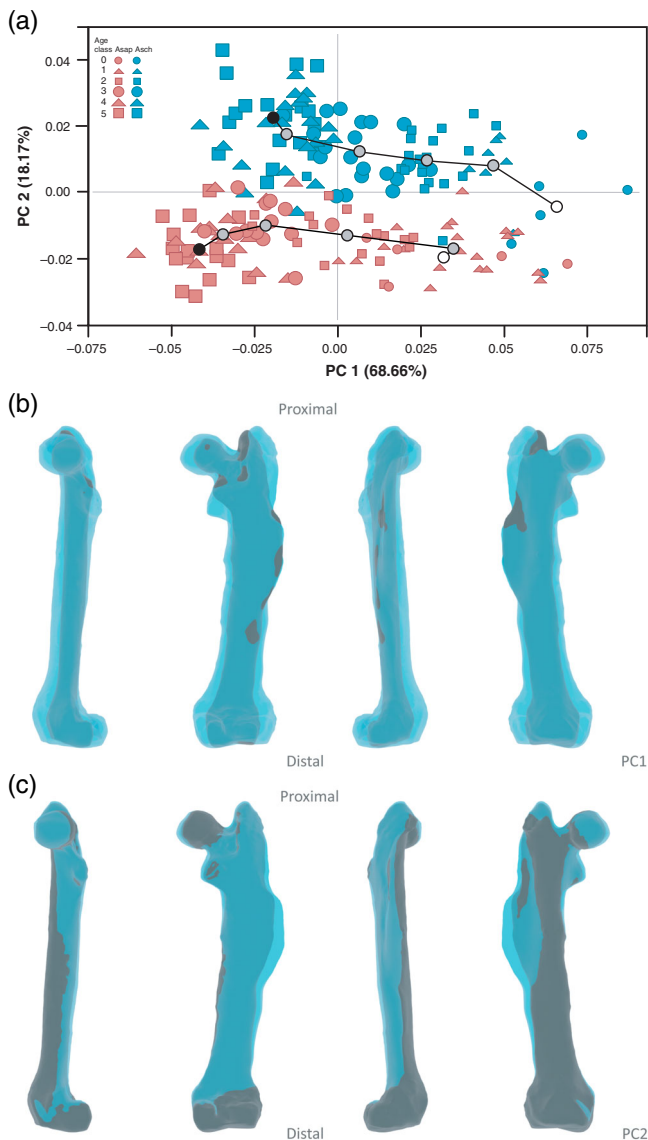
FIGURE 5 Ontogenetic phenotypic trajectories of *Arvicola sapidus* and *Arvicola scherman* derived from the phenotypic trajectory analysis. (a) Shape trajectories projected onto the first two principal components (PC1 and PC2) (based on covariance matrix of group means). White dots represent the beginning (age class 0) and the black dots the end (age class 5) of the trajectories. The lines define the trajectories and the larger dots to the mean of each age class. (b, c) Shape changes associated with each extreme of the first two principal components; gray, negative extreme of the axis; blue, positive extreme of the axis. Bones are represented from left to right in medial, caudal, lateral, and cranial views

Wilson & Sánchez-Villagra, 2010). Our results suggest that ontogeny may be more flexible than previously thought and that locomotion mode is an important selective force modelling the allometric trajectory of the involved bones. The different functional pressures exerted on the femur in the two studied species may have led to phenotypic variation and consequently to differences between the corresponding allometric trajectories.

In all age classes, the shape of the femur differed significantly between *A. sapidus* and *A. scherman*. Their phenotypic trajectories showed a different direction, indicating that not only the shape of the bone differs in each age class, but also that shape changes occurring during postnatal ontogeny are not concordant in the two species. The angle between phenotypic trajectories was quite similar to that observed in the allometric trajectories, which may suggest that a significant amount of the variation in femur shape is allometric. Similar results were also reported for the mandible of these species (Durão et al., 2019). In the humerus, in addition to the interspecific differences in the direction of the corresponding phenotypic trajectories, the length of these was also significantly different between both taxa, evidencing a larger shape change during the postnatal growth of this bone in *A. scherman* than in *A. sapidus* (Durão et al., 2020). The relative amount of shape variation explained by the factor species was also greater in the humerus than in the femur (compare results from Table 4 with those of table 4 in Durão et al., 2020). As results of the PCAs revealed, while in the humerus, differences between species were mainly explained by PC1, which accounted for 31% of total shape variation (Durão et al., 2020) in the femur differences between species were mostly explained by PC2, which accounted for less than 12% of the total shape variation. These results seem to indicate that functional pressures are related to the type of locomotion and that, depending on the role of each bone, the shape changes occurring during ontogeny may be more or less pronounced. The more marked shape changes of the humerus during postnatal ontogeny are concurrent with the prominent action of this bone in the digging process, and with the fact that this is a biomechanically and energetically very demanding activity (White, 2005).

In semiaquatic animals, relatively major morphological changes in the distal bones of hindlimbs are expected, taking into account their involvement in producing propulsive forces during swimming (Samuels & Valkenburgh, 2008). To test this hypothesis, it would be interesting, for example, to perform comparative morphological analyses by means of geometric morphometrics on the postnatal ontogeny of the tibia in fossorial and semiaquatic water voles, especially bearing in mind that certain evolutionary changes in the form of this bone have been reported in *Arvicola* by using linear measurements (Cubo et al., 2006).

4.3 | Biomechanical consequences of femur shape

Locomotion imposes strong demands on the musculoskeletal system, which may affect bone morphology and

the organization of attached musculature (Biewener & Patek, 2018). Our results on the femur of *A. sapidus* and *A. scherman* show that the morphological distances between these species were significantly different in all age classes. Distances were greater in the nonallometric shape data than shape data, which reveal that these taxa shared part of allometric shape changes. Several interspecific differences in the adult femur shape were also observed, the most conspicuous being the extension of the greater and third trochanter, and the position of the *fovea capitis*.

4.3.1 | Fossorial locomotion

The morphology of the third trochanter is highly variable in the mammalian femur, in terms of its presence/absence, lateral expansion, and proximo-distal length (Salton & Sargis, 2009). Both *A. scherman* and *A. sapidus* show this tubercle but in the former species, it is wider and much distal. As described for example in the capybara (*Hydrochoerus hydrochaeris*), in this part of the femur inserts the gluteus superficialis muscle (García-Esponda & Candela, 2016), which originates from the lumbodorsal fascia and that helps flex the hip joint. As has been reported for several mammal species, the mass of this muscle seems to have noticeable effects on the size, position, and shape of the third trochanter (Anemone & Covert, 2000; García-Esponda & Candela, 2016; Salton & Sargis, 2009; Sargis, 2002; Smith & Savage, 1956). In particular, a wider third trochanter is linked to the powerful development of the gluteus superficialis muscle (Smith & Savage, 1956). This feature may provide a mechanical advantage because it increases the efficiency of the moment arm as well as provides a great lever for gluteus superficialis muscle (Salton & Sargis, 2009; Sargis, 2002). A robust third trochanter also contributes to the hip stabilization during the extension of the leg and may be reduced bending stresses. This trait has also been found in other fossorial mammals (Salton & Sargis, 2009), such as the Hispaniolan solenodon (*Solenodon paradoxus*), the mole-like rice tenrec (*Oryzorictes hova*), the four-toed rice tenrec (*Oryzorictes tetradactylus*), and the naked mole-rat (*Heterocephalus glaber*). As suggested by Salton and Sargis (2009), the sturdiness of this trochanter permits a powerful thigh extension with some abduction, action related to throwing back the loose earth to kicking it out of the burrow. Since in *A. scherman* the hindlimbs play a relatively important role in the digging process (Airoldi et al., 1976; Laville, 1989, 1989b), a stronger flex of the hip could be linked to the corresponding mechanical requirement.

The lesser trochanter of *A. scherman* is oriented postero-medially and is larger than in *A. sapidus*. Similar morphological features than we have observed in *A. scherman* had already been described in other diggers, such as species of the genus *Tympanoctomys*, scratch-digger/chisel-tooth diggers (Pérez, Barquez, & Díaz, 2017), and representatives of the family Bathyergidae (Sahd, Bennett, & Hotzé, 2019). This trochanter provides the insertion site for the iliopsoas complex, the strongest flexor of the hip, that has an important function in standing, walking, and running, namely in the recovery phase. In *A. scherman*, the well-developed lesser trochanter could indicate a large insertion area for this complex. Its postero-medial protraction could be related to para-sagittal movements and a strong lateral rotation of the femur considering that the medial position of the lesser trochanter increases the lever arm for the iliopsoas muscle (Argot, 2002; Taylor, 1976; Toledo, Bargo, & Vizcaíno, 2015). *Arvicola scherman* also shows a slight variation on the femur head angle in relation to *A. sapidus*, being more medially in the latter species. These differences could be linked to the restricted planes of motion (Anemone & Covert, 2000; Salton & Sargis, 2009; Szalay & Sargis, 2001) and consequently associated with differences in hip mobility between the two species. The femur of *A. scherman* exhibits a cranial-medial shift of the *fovea capitis* related to *A. sapidus*. In this dimple attach the teres femoris ligament, one of the large ligaments that connect the femoral head to the hip. The relatively great extension of the *fovea capitis* in *A. scherman* suggests a strong ligament and a greater stabilization of the hip and knee. The general morphology of the lesser trochanter in *A. scherman* is consistent with the ability for extension and flexion of the hip as well as, abduction and external rotation of the femur. These movements are favored by the presence of a strong ligament that helps to stabilize the hip when vigorously kicks. In turn, the medial position of the femur head in *A. scherman* may limit hip mobility at parasagittal motion, while maintaining the capacity for extension and flexion. These morphological characteristics in *A. scherman* are probably related to the digging process, specifically, to the soil removal, in which the angle between the pelvis and the femur diminishes, and the hip is extended backward to sweep loose soil farther away from the burrow.

Another distinctive feature of *A. scherman* with respect to *A. sapidus* is the existence of a more robust femur, which is congruent with the results published in previous studies based on linear measurements (Cubo et al., 2006; Ventura, 1988, 1990, 1992). This typical trait of fossorial rodents (Biknevicius, 1993; Casinos, Quintana, & Viladiu, 1993; Samuels & Valkenburgh, 2008; Wilson & Geiger, 2015) is related to withstand the bending and torsion forces placed on the limbs during the digging process (Biknevicius, 1993; Stein, 2000). The

robustness of the femur in *A. scherman* likely results from both the support that the bone needs for the development of muscles and as a response to the mechanical stress that hindlimbs are continuously subjected to. Compared to *A. sapidus*, *A. scherman* exhibits a wide distal epicondyle which provides a great surface area for the insertion of the gastrocnemius and soleus muscles, plantar flexors of the foot (García-Esponda & Candela, 2016). The increase in the epicondylar area may aid in resisting the tendency of the body to be pushed backward while digging, as suggested by Samuels and Valkenburgh (2008) for other chisel-tooth digger rodents species (Bathyergids and Spalacids).

4.3.2 | Aquatic locomotion

Swimming imposes challenges for semiaquatic species because water is a dense and viscous medium that establishes a strong hydrodynamic demand on the musculoskeletal system (Gillis & Blob, 2001). This requirement can lead to morphological changes that allow improving locomotor performance and stability, such as increased speed, drag reduction, improved thrust output, and increased maneuverability (Fish, 2016; Fish & Stein, 1991 and references therein). Different adaptations of the hindlimbs seem to have been developed by different quadrupedal paddling mammals with semiaquatic habits (Botton-Divet, Cornette, Fabre, Herrel, & Houssaye, 2016; García-Esponda & Candela, 2016; Stein, 1988). These morphological changes seem to be related to the amount of time spent by the animal in water, and to the activities performed there (Dunstone, 1979; Stein, 1988). Semiaquatic animals, due to their great dependence on land once compared to their terrestrial relatives, display few or absent limb specializations (García-Esponda & Candela, 2016; Thewissen & Taylor, 2007). This moderate morphological variation appears to be associated with functional needs both on land and in water (Stein, 1989). As for *Arvicola*, we observed that *A. sapidus* shows, in comparison with *A. scherman*, a slight medial-cranial extension of the greater trochanter. This tubercle provides the insertion area for the gluteus piriformis and medius muscles, both extensors and abductors of the hip joint (García-Esponda & Candela, 2016). The modest expansion of the greater trochanter in *A. sapidus* could be related to the relative size increase of the gluteus medius muscle, feature also found in other semiaquatic rodent species (Candela & Picasso, 2008; Stein, 1988). This muscle is involved in rapid movement toward the end of the stroke (Smith & Savage, 1956). As suggested by Stein (1988), the size increase of the gluteus medius muscle allows decreasing the resistance to water, maintaining the impulse after starting the power phase. This morpho-functional relationship remains to be tested in *A. sapidus*.

5 | CONCLUSIONS

Results obtained in the present study reveal a combination of phylogenetic and functional signals in the postnatal growth of the femur in *A. sapidus* and *A. scherman*. On the one hand, shared common traits between these taxa were found, which can be considered traces of their common origin. On the other hand, we found evidence that certain variations in the femur shape and particular differences in allometric and phenotypic trajectories between these taxa are associated with their different types of locomotion. Our study emphasizes the importance of developing comparative studies in closely related species to assess to which extent functional and phylogenetic factors affect the growth patterns of bones involved in locomotion. As for genus *Arvicola* in particular, it would be interesting to extend this kind of studies to other semiaquatic or fossorial water vole populations, and even others that can change the type of locomotion according to the reproduction cycle and/or the environmental conditions (Barreto & MacDonald, 2000; Kratochvíl & Grulich, 1961; Potapov, Nazarova, Muzyka, Potapova, & Evsikov, 2012; Stewart, Jarrett, Scott, White, & McCafferty, 2019; Telfer et al., 2003).

CONFLICT OF INTEREST
The authors declare no potential conflicts of interest.

AUTHOR CONTRIBUTIONS
Ana Filipa Durão: Formal analysis (lead); investigation (lead); methodology (equal); visualization (lead); writing – original draft (lead). **Francesc Muñoz-Muñoz:** Conceptualization (equal); methodology (equal); writing – review and editing (equal). **Jacint Ventura:** Conceptualization (equal); resources (lead); supervision (lead); writing – review and editing (equal).

DATA AVAILABILITY STATEMENT
The data generated by this study are available in the Zenodo repository (10.5281/zenodo.5155457).

ORCID

Ana Filipa Durão https://orcid.org/0000-0003-0859-5371

Francesc Muñoz-Muñoz https://orcid.org/0000-0003-2084-0368

Jacint Ventura https://orcid.org/0000-0001-7527-1532

REFERENCES

Adams, D. C., & Collyer, M. L. (2007). Analysis of character divergence along environmental gradients and other covariates. *Evolution*, *61*, 510–515.

Adams, D. C., & Collyer, M. L. (2009). A general framework for the analysis of phenotypic trajectories in evolutionary studies. *Evolution*, *63*, 1143–1154.

Adams, D. C., & Nistri, A. (2010). Ontogenetic convergence and evolution of foot morphology in European cave salamanders (Family: Plethodontidae). *BMC Evolutionary Biology*, *10*, 216.

Adams, D. C., Collyer, M. L., Kaliontzopoulou, A., & Sherratt, E. (2017). Geomorph: Software for geometric morphometric analyses. R package version 3.0.5.

Airoldi, J. P. (1976). Le terrier de la forme fouisseuse du campagnol terrestre (*Arvicola terrestris scherman* Shaw) (Mammalia, Rodentia). *Zeitschrift für Säugetierkunde*, *41*, 23–42.

Airoldi, J. P., Altrocchi, R., & Meylan, A. (1976). Le comportement fouisseur du campagnol terrestre, *Arvicola terrestris scherman* Shaw (Mammalia, Rodentia). *Revue Suisse Zoologie*, *83*, 282–286.

Airoldi, J. P., & De Werra, D. (1993). The burrow system of the fossorial form of the water vole (*Arvicola terrestris scherman* Shaw) (Mammalia, Rodentia): An approach using graph theoretical methods and simulation models. *Mammalia*, *57*, 423–433.

Anemone, R. L., & Covert, H. H. (2000). New skeletal remains of Omomys (Primates, Omomyidae): Functional morphology of the hindlimb and locomotor behavior of a Middle Eocene primate. *Journal of Human Evolution*, *38*, 607–633.

Argot, C. (2002). Functional-adaptive analysis of the hindlimb anatomy of extant marsupials and the paleobiology of the Paleocene marsupials *Mayulestes ferox* and *Pucadelphys andinus*. *Journal of Morphology*, *256*, 76–108.

Barreto, G. R., & MacDonald, D. W. (2000). The decline and local extinction of a population of water voles, *Arvicola terrestris*, in southern England. *Zeitschrift Für Säugetierkunde*, *65*, 110–120.

Biewener, A. A., & Patek, S. N. (2018). *Animal locomotion*. Oxford: Oxford University Press.

Biknevicius, A. R. (1993). Biomechanical scaling of limb bones and differential limb use in caviomorph rodents. *Journal of Mammalogy*, *74*, 95–107.

Bookstein, F. L. (1991). *Morphometric tools for landmark data: Geometry and biology*. New York, NY: University Press.

Botton-Divet, L., Cornette, R., Fabre, A., Herrel, A., & Houssaye, A. (2016). Morphological analysis of long bones in semi-aquatic mustelids and their terrestrial relatives. *Integrative and Comparative Biology*, *56*, 1298–1309.

Candela, A. M., & Picasso, B. J. (2008). Functional anatomy of the limbs of Erethizontidae (rodentia, caviomorpha): Indicators of locomotor behavior in Miocene porcupines. *Journal of Morphology*, *269*, 552–593.

Carrier, D. R. (1983). Postnatal ontogeny of the musculo-skeletal system in the black-tailed jack rabbit (*Lepus californicus*). *Journal of Zoology*, *201*, 27–55.

Casinos, A., Quintana, C., & Viladiu, C. (1993). Allometry and adaptation in the long bones of a digging group of rodents (Ctenomyinae). *Zoological Journal of the Linnean Society*, *107*, 107–115.

Chevret, P., Renaud, S., Helvaci, Z., Ulrich, R. G., Quéré, J., & Michaux, J. R. (2020). Genetic structure, ecological versatility, and skull shape differentiation in *Arvicola* water voles (Rodentia, Cricetidae). *Journal of Zoology Systematics and Evolutionary Research*, *58*, 1323–1334.

Collyer, M. L., & Adams, D. C. (2007). Analysis of two-state multivariate phenotypic change in ecological studies. *Ecology*, *88*, 683–692.

Collyer, M. L., & Adams, D. C. (2013). Phenotypic trajectory analysis: Comparison of shape change patterns in evolution and ecology. *Hystrix*, *24*, 75–83.

Collyer, M. L., Sekora, D. J., & Adams, D. C. (2015). A method for analysis of phenotypic change for phenotypes described by high-dimensional data. *Heredity*, *115*, 357–365.

Collyer, M. L., & Adams, D. C. (2018). RRPP: An r package for fitting linear models to high-dimensional data using residual randomization. *Methods in Ecology and Evolution*, *9*, 1772–1779.

Cubo, J., Ventura, J., & Casinos, A. (2006). A heterochronic interpretation of the origin of digging adaptations in the northern water vole, *Arvicola terrestris* (Rodentia: Arvicolidae). *Biological Journal of the Linnean Society*, *87*, 381–391.

Dryden, I., & Mardia, K. V. (1998). *Statistical shape analysis*. Chichester, England: Wiley.

Dunstone, N. (1979). Swimming and diving behavior of the mink (*Mustela vison* Schreber). *Carnivore*, *2*, 56–61.

Durão, A. F., Muñoz-Muñoz, F., Martínez-Vargas, J., & Ventura, J. (2018). Obtaining three-dimensional models of limb long bones from small mammals: A photogrammetric approach. In C. Rissech, L. Lloveras, J. Nadal, & J. M. Fullola (Eds.), *Geometric morphometrics. Trends in biology, paleobiology and archaeology* (pp. 125–138). Barcelona, Spain: SERP - Universitat Barcelona.

Durão, A. F., Ventura, J., & Muñoz-Muñoz, F. (2019). Comparative post-weaning ontogeny of the mandible in fossorial and semi-aquatic water voles. *Mammalian Biology*, *97*, 95–103.

Durão, A. F., Muñoz-Muñoz, F., & Ventura, J. (2020). Three-dimensional geometric morphometric analysis of the humerus: Comparative postweaning ontogeny between fossorial and semiaquatic water voles (*Arvicola*). *Journal of Morphology*, *281*, 1679–1692.

Echeverría, A. I., Becerra, F., & Vassallo, I. (2014). Postnatal ontogeny of limb proportions and functional indices in the subterranean rodent *Ctenomys talarum* (Rodentia: Ctenomyidae). *Journal of Morphology*, *275*, 902–913.

Elissamburu, A., & Vizcaíno, S. F. (2004). Limb proportions and adaptations in caviomorph rodents (Rodentia: Caviomorpha). *Journal of Zoology*, *262*, 145–159.

Enlow, D. H. (1962). A study of the post-natal growth and remodeling of bone. *American Journal of Anatomy*, *110*, 79–101.

EOS Systems Inc. (2015). *Photomodeler Scanner (v2015.1.1)*. Vancouver, Canada: EOS Systems.

Esquerré, D., Sherratt, E., & Keogh, J. S. (2017). Evolution of extreme ontogenetic allometric diversity and heterochrony in pythons, a clade of giant and dwarf snakes. *Evolution*, *71*, 2829–2844.

Falkingham, P. L. (2012). Acquisition of high resolution 3D models using free, open-source, photogrammetric software. *Palaeontologia Electronica*, *15*, 1–15.

Fish, F. E., & Stein, B. R. (1991). Functional correlates of differences in bone density among terrestrial and aquatic genera in the family Mustelidae (Mammalia). *Zoomorphology*, *110*, 339–345.

Fish, F. E. (2016). Secondary evolution of aquatic propulsion in higher vertebrates: Validation and prospect. *Integrative and Comparative Biology*, *56*, 1285–1297.

García, G. J. M., & da Silva, J. K. L. (2006). Interspecific allometry of bone dimensions: A review of the theoretical models. *Physics of Life Reviews*, *3*, 188–209.

García-Esponda, C. M., & Candela, A. M. (2016). Hindlimb musculature of the largest living rodent *Hydrochoerus hydrochaeris* (Caviomorpha): Adaptations to semiaquatic and terrestrial styles of life. *Journal of Morphology*, *277*, 286–305.

Garde, J. M. (1992). *Biología de la rata de agua Arvicola sapidus Miller, 1908 (Rodentia, Arvicolidae) en el sur de Navarra (España)*. (PhD thesis). Universidad de Navarra, Navarra.

Garde, J., Escala, M. C., & Ventura, J. (1993). Determinación de la edad relativa en la rata de agua meridional, *Arvicola sapidus* Miller, 1908 (Rodentia, Arvicolidae). *Doñana, Acta Vertebrata*, *20*, 266–276.

Gillis, G. B., & Blob, R. W. (2001). How muscles accommodate movement in different physical environments: Aquatic vs terrestrial locomotion in vertebrates. *Comparative Biochemistry and Physiology - Part A*, *131*, 61–75.

Goodall, C. (1991). Procrustes methods in the statistical analysis of shape. *Journal of the Royal Statistical Society*, *53*, 285–339.

Gould, S. J. (1966). Allometry and size in ontogeny and phylogeny. *Biological Reviews*, *41*, 587–640.

Gray, J. A., Sherratt, E., Hutchinson, M. N., & Jones, M. E. H. (2019). Changes in ontogenetic patterns facilitate diversification in skull shape of Australian agamid lizards. *BMC Evolutionary Biology*, *19*, 1–10.

Hart, N. H., Nimphius, S., Rantalainen, T., Ireland, A., Siafrikas, A., & Newton, R. U. (2017). Mechanical basis of bone strength: Influence of bone material, bone structure and muscle action. *Journal of Musculoskeletal and Neuronal Interaction*, *17*, 114–139.

Hildebrand, M. (1985). Digging of quadrupeds. In M. Hildebrand, D. M. Bramble, K. F. Liem, & D. B. Wake (Eds.), *Functional vertebrate morphology* (pp. 89–109). Cambridge, MA: Belknap Press.

Klingenberg, C. P. (2011). MorphoJ: An integrated software package for geometric morphometrics. *Molecular Ecology Resources*, *11*, 353–357.

Klingenberg, C. P. (2016). Size, shape, and form: Concepts of allometry in geometric morphometrics. *Development Genes and Evolution*, *226*, 113–137.

Kratochvíl, J., & Grulich, I. (1961). On the distribution and habitat requeriments in the water-vole *Arvicola terrestris*, in Czechoslovakia. *Zoologicke Listy*, *10*, 265–280.

Kryštufek, B., Koren, T., Engelberger, S., Horváth, G. F., Purger, J. J., Arslan, A., ... Murariu, D. (2015). Fossorial morphotype does not make a species in water voles. *Mammalia*, *79*, 293–303.

Laville, E. (1989). Etude cinématique du fouissage chez *Arvicola terrestris scherman* (Rodentia, Arvicolidae). *Mammalia*, *53*, 177–190.

Laville, E. (1989b). Etude morphofonctionelle comparative des structures osseuses impliquées dans le fouissage d'*Arvicola terrestris scherman* (Rodentia, Arvicolidae). *Canadian Journal of Zoology*, *68*, 2437–2444.

Laville, E., Casinos, A., Gasc, J. P., Renous, S., & Bou, J. (1989). Les mécanismes du fouissage chez *Arvicola terrestris* et *Spalax ehrenbergi*: étude fonctionelle et évolutive. *Anatomischer Anzeiger*, *169*, 131–144.

Lehmann, W. H. (1963). The forelimb architecture of some fossorial rodents. *Journal of Morphology*, *113*, 59–76.

Lessa, E. P., Vassallo, A. I., Verzi, D. H., & Mora, M. S. (2008). Evolution of morphological adaptations for digging in living and extinct ctenomyid and octodontid rodents. *Biological Journal of the Linnean Society*, *95*, 267–283.

Mahmoudi, A., Maul, L. C., Khoshyar, M., Darvish, J., Aliabadian, M., & Kryštufek, B. (2020). Evolutionary history of water voles revisited: Confronting a new phylogenetic model from molecular data with the fossil record. *Mammalia*, *84*, 171–184.

Mate, I., Barrull, J., Salicrú, M., Ruiz-Olmo, J., & Gosàlbez, J. (2013). Habitat selection by southern water vole (*Arvicola sapidus*) in riparian environments of Mediterranean mountain areas: A conservation tool for the species. *Acta Theriologica*, *58*, 25–37.

Monteiro, L. (1999). Multivariate regression models and geometric morphometrics: The search for causal factors in the analysis of shape. *Systematic Biology*, *48*, 192–199.

Montoya-Sanhueza, G., & Chinsamy, A. (2018). Cortical bone adaptation and mineral mobilization in the subterranean mammal *Bathyergus suillus* (Rodentia: Bathyergidae): Effects of age and sex. *PeerJ*, *6*, e4944.

Montoya-Sanhueza, G., Wilson, L. A. B., & Chinsamy, A. (2019). Postnatal development of the largest subterranean mammal (*Bathyergus suillus*): Morphology, osteogenesis and modularity of the appendicular skeleton. *Developmental Dynamics*, *248*, 1101–1128.

Musser, G. G., & Carleton, M. C. (2005). *Arvicola* Lacépède, 1799; *Arvicola amphibius* (Linnaeus, 1758); *Arvicola sapidus* Miller, 1908; *Arvicola scherman* (Shaw, 1801). In D. E. Wilson & D. M. Reeder (Eds.), *Mammal species of the world. A taxonomic and geographic reference* (pp. 963–966). Baltimore, MD: Johns Hopkins University Press.

Pardiñas, U. F. J., Myers, P., León-Paniagua, L., Ordóñez-Garza, N., Cook, J. A., Kryštufek, B., ... Patton, J. L. (2017). Family Cricetidae (true hamsters, voles, lemmings and new world rats and mice). In D. E. Wilson, T. E. Lacher, Jr., & R. A. Mittermeier (Eds.), *Handbook of the mammals of the world. Vol. 7. Rodents II* (pp. 204–535). Lynx Edicions: Barcelona, Spain.

Pérez, M. J., Barquez, R. M., & Díaz, M. M. (2017). Morphology of the limbs in the semi-fossorial desert rodent species of *Tympanoctomys* (Octodontidae, Rodentia). *ZooKeys*, *710*, 77–96.

Potapov, M. A., Nazarova, G. G., Muzyka, V. Y., Potapova, O. F., & Evsikov, V. I. (2012). Extrisic and intrinsic factors of regulations of reproductive potential in the water vole (*Arvicola amphibius*) population from western Siberia. In A. Triunveri & D. Scalise (Eds.), *Rodents - Habitats, pathology and environmental impact* (pp. 23–41). New York, NY: Nova Science Publishers.

Quéré, J., & Le Louarn, H. (2011). *Les rongeurs de France. Faunistique et biologie*. Versailles, France: Éditions Quae.

R Development Core Team (2016). *R: A language and environment for statistical computing. Version 3.5.1*. Vienna, Austria: R Foundation for Statistical Computing Retrieved from www.R-project.og

Rice, W. R. (1989). Analyzing tables of statistical tests. *Evolution*, *43*, 223–225.

Reichstein, H. (1963). Beitrag zur systematischen Gliederung des Genus *Arvicola* Lacépède 1799. *Zeitschrift für Zoologische Systematik und Evolutionsforschung*, *1*, 155–204.

Reichstein, H. (1982). Gattung *Arvicola* Lacépède 1799 Schermäuse. In J. Niethammer & F. Krapp (Eds.), *Handbuch der Säugetiere Europas Vol. 2 / 1* (pp. 209–252). Akademische Verlagsgesellschaft: Wiesbaden, Germany.

Rohlf, F. J., & Slice, D. (1990). Extensions of the Procrustes method for the optimal superimposition of landmarks. *Systematic Zoology*, *39*, 40–59.

Sahd, L., Bennett, N. C., & Hotzé, S. H. (2019). Hind foot drumming: Morphological adaptations of the muscles and bones of the hind limb in three African mole-rat species. *Journal of Anatomy*, 235, 811–824.

Salton, J. A., & Sargis, E. J. (2009). Evolutionary morphology of the tenrecoidea (Mammalia) hindlimb skeleton. *Journal of Morphology*, 270, 367–387.

Samuels, J. X., & Valkenburgh, B. V. (2008). Skeletal indicators of locomotor adaptations in living and extinct rodents. *Journal of Morphology*, 269, 1387–1411.

Samuels, J. X., Meachen, J. A., & Sakai, S. A. (2013). Postcranial morphology and the locomotor habits of living and extinct carnivorans. *Journal of Morphology*, 274, 121–146.

Sargis, E. J. (2002). Functional morphology of the hindlimb of Tupaiids (Mammalia, Scandentia) and its phylogenetic implications. *Journal of Morphology*, 254, 149–185.

Serrat, M. A., Lovejoy, C. O., & King, D. (2007). Age- and site-specific decline in insulin-like growth factor-I receptor expression is correlated with differential growth plate activity in the mouse hindlimb. *The Anatomical Record: Advances in Integrative Anatomy and Evolutionary Biology*, 290, 375–381.

Smith, J. M., & Savage, R. J. G. (1956). Some locomotory adaptations in mammals. *Zoological Journal of the Linnean Society*, 42, 603–622.

StatSoft. (2014). *Statistica (data analysis software system). Version 12*. Tulsa, OK: Author.

Stein, B. R. (1988). Morphology and allometry in several genera of semiaquatic rodents (*Ondatra*, *Nectomys*, and *Oryzomys*). *Journal of Mammalogy*, 69, 500–511.

Stein, B. R. (1989). Bone density and adaptation in semiaquatic mammals. *Journal of Mammalogy*, 70, 467–476.

Stein, B. R. (1993). Comparative hind limb morphology in Geomyine and Thomomyine pocket gophers. *Journal of Mammalogy*, 74, 86–94.

Stein, B. R. (2000). Morphology of subterranean rodents. In E. A. Lacey, J. L. Patton, & G. N. Cameron (Eds.), *Life underground: The biology of subterranean mammals* (pp. 19–61). Chicago, CA: University of Chicago Press.

Stewart, R. A., Jarrett, C., Scott, C., White, S. A., & McCafferty, D. J. (2019). Water vole (*Arvicola amphibius*) abundance in grassland habitats of Glasgow. *The Glasgow Naturalist*, 27, 10–19.

Szalay, F. S., & Sargis, E. J. (2001). Model-based analysis of postcranial osteology of marsupials from the Palaeocene of Itaboraí (Brazil) and the phylogenetics and biogeography of Metatheria. *Geodiversitas*, 23, 139–302.

Taylor, M. E. (1976). The functional antomy of the hindlimbs of some African Viverridae (Carnivora). *Journal of Morphology*, 148, 227–254.

Telfer, S., Dallas, J. F., Aars, J., Piertney, S. B., Stewart, W. A., & Lambin, X. (2003). Demographic and genetic structure of fossorial water voles (*Arvicola terrestris*) on Scottish islands. *Journal of Zoology*, 259, 23–29.

Thewissen, J. G. M., & Taylor, M. A. (2007). Aquatic adaptations in the limbs of amniotes. In B. K. Hall (Ed.), *Fins into limbs - Evolution, development, and transformation* (pp. 310–322). Chicago, CA: The University of Chicago Press.

Toledo, N., Bargo, M. S., & Vizcaíno, S. F. (2015). Muscular reconstruction and functional morphology of the hind limb of santacrucian (Early Miocene) sloths (Xenarthra, Folivora) of Patagonia. *The Anatomical Records*, 298, 842–864.

Vassallo, A. I. (1998). Functional morphology, comparative behaviour, and adaptation in two sympatric subterranean rodents genus *Ctenomys* (Caviomorpha: Octodontidae). *Journal of Zoology*, 244, 415–427.

Ventura, J. (1988). *Contribución al conocimiento del género Arvicola Lacépède, 1799, en el nordeste de la Peninsula Ibérica*. (PhD thesis). Universidad de Barcelona, Barcelona.

Ventura, J. (1990). Datos biométricos sobre los huesos largos y la escápula de *Arvicola sapidus* Miller, 1908 (Rodentia, Arvicolidae). *Boletín de la Real Sociedad Española de Historia Natural (Sección Biológica)*, 86, 1–4.

Ventura, J. (1992). Morphometric data on the scapula and limb long bones of *Arvicola terrestris* (Linnaeus, 1758) (Rodentia, Arvicolidae). *Revue Suisse Zoologie*, 99, 629–636.

Ventura, J. (1993). Crecimiento relativo de *Arvicola terrestris monticola* (Rodentia, Arvicolidae). *Miscellania Zoológica*, 17, 237–248.

Ventura, J. (2007). *Arvicola terrestris* (Linnaeus, 1758); *Arvicola sapidus* Miller, 1908. In L. J. Palomo, J. Gisbert, & J. C. Blanco (Eds.), *Atlas y Libro Rojo de los Mamíferos Terrestres de España* (pp. 401–407). Madrid, Spain: Dirección General para la Biodiversidad -SECEM-SECEMU.

Ventura, J., & Gosálbez, J. (1992). Criterios para la determinación de la edad relativa en *Arvicola terrestris monticola* (Rodentia, Arvicolidae). *Miscellania Zoológica*, 16, 197–206.

Ventura, J., & Casado-Cruz, M. (2011). Post-weaning ontogeny of the mandible in fossorial water voles: Ecological and evolutionary implications. *Acta Zoologica*, 92, 12–20.

Vleck, D. (1979). The energy cost of burrowing by the pocket gopher *Thomomys bottae*. *Physiological Zoology*, 52, 122–136.

Voje, K. L., Hansen, T. F., Egset, C. K., Bolstad, G. H., & Pélabon, C. (2013). Allometric constraints and the evolution of allometry. *Evolution*, 68, 866–885.

White, C. R. (2005). The allometry of burrow geometry. *Journal of Zoology*, 265, 395–403.

Wilson, L. A. B., & Sánchez-Villagra, M. R. (2010). Diversity trends and their ontogenetic basis: An exploration of allometric disparity in rodents. *Proceedings of the Royal Society*, 277, 1227–1234.

Wilson, L. A. B., & Geiger, M. (2015). Diversity and evolution of femoral variation in Ctenohystrica. In P. G. Cox & L. Hautier (Eds.), *Evolution of the rodents: Advances in phylogeny, functional morphology, and development* (pp. 510–538). Cambridge, MA: Cambridge University Press.

Young, J. W., Férnandez, D., & Fleagle, J. G. (2010). Ontogeny of long bone geometry in capuchin monkeys (*Cebus albifrons* and *Cebus apella*): Implications for locomotor development and life history. *Biology Letters*, 6, 197–200.

SUPPORTING INFORMATION